Structural basis for NKG2A/CD94 recognition of HLA-E

Brett K. Kaiser, Juan Carlos Pizarro*, Julie Kerns, and Roland K. Strong†

Division of Basic Sciences, Fred Hutchinson Cancer Research Center, 1100 Fairview Avenue North, Seattle, WA 98109

Communicated by Pamela J. Bjorkman, California Institute of Technology, Pasadena, CA, March 19, 2008 (received for review March 11, 2008)

The NKG2x/CD94 (x = A, C, E) natural killer-cell receptors perform an important role in immunosurveillance by binding to HLA-E complexes that exclusively present peptides derived from MHC class I leader sequences, thereby monitoring MHC class I expression. We have determined the crystal structure of the NKG2A/CD94/HLA-E complex at 4.4-Å resolution, revealing two critical aspects of this interaction. First, the C-terminal region of the peptide, which displays the most variability among class I leader sequences, interacts entirely with CD94, the invariant component of these receptors. Second, residues 167–170 of NKG2A/C account for the ≈6-fold-higher affinity of the inhibitory NKG2A/CD94 receptor compared to its activating NKG2C/CD94 counterpart. These residues do not contact HLA-E or peptide directly but instead form part of the heterodimer interface with CD94. An evolutionary analysis across primates reveals that whereas CD94 is evolving under purifying selection, both NKG2A and NKG2C are evolving under positive selection. Specifically, residues at the CD94 interface have evolved under positive selection, suggesting that the evolution of these genes is driven by an interaction with pathogen-derived ligands. Consistent with this possibility, we show that NKG2C/CD94, but not NKG2A/CD94, weakly but specifically binds to the CMV MHC-homologue UL18. Thus, the evolution of the NKG2x/CD94 family of receptors has likely been shaped both by the need to bind the invariant HLA-E ligand and the need to avoid subversion by pathogen-derived decoys.

crystallography | immunology | immunoreceptors | NKG2A

Natural killer (NK) cells complement adaptive T cell responses by monitoring other cells for the normal expression of classical MHC class I proteins, often dysregulated during viral infection and neoplastic transformation. Human NK cells express two major classes of class I-specific receptors (1). The killer inhibitory receptor (KIR) family, consisting of 11 highly polymorphic receptors that use two or three tandem Ig-superfamily domains in their ectodomains, binds directly to classical MHC molecules. The NKG2x/CD94 receptors (x = A/B, C, E/H, where A/B and E/H are splice variants) contain C-type lectin-like (CTLD) ectodomains and bind to the nonclassical MHC protein HLA-E, which presents peptides derived from the relatively conserved leader sequences of classical MHC proteins and HLA-G (2, 3).

Although NKG2x/CD94 receptors bind to the common ligand HLA-E, different members of the family can transmit opposing signals via their intracellular domains. NKG2A/CD94 functions as an inhibitory receptor by signaling through two inhibitory ITIM motifs (V/IxYxxL/V), whereas NKG2C/CD94 functions as an activating receptor by associating with the DAP12 signaling adapter. How NK cells integrate multiple opposing signals into a single output (kill or tolerate) is not well understood, although it is generally thought that inhibitory signals predominate. Perhaps enabling this dominance, NKG2A/CD94 binds to HLA-E complexes with affinities consistently 6-fold stronger than NKG2C/CD94 (4). This trend has also seen in other NK receptor families with paired stimulatory/inhibitory receptors, including the KIR and Ly49 families. It has been proposed that some activating receptors may have evolved to bind pathogen-derived ligands directly, but only one example has been firmly established: the recognition of mCMV m157 by murine Ly49H (5, 6).

HLA-E is highly homologous to classical MHC proteins but has acquired critical changes that restrict the repertoire of peptides it binds to nonamers derived from the leader sequences of classical MHC (3, 7–10). The HLA allele from which the nonamer peptide is derived significantly influences the strength of interaction with the NKG2x/CD94 receptor, despite single, conserved substitutions in most cases (3, 4, 8, 11, 12). The importance of HLA-E in viral surveillance is underscored by the fact that it is targeted for subversion by the CMV protein gpUL40, which contains the HLA-E peptide sequence VMAPRTLIL within its leader sequence (13, 14).

Previous studies have not conclusively determined how NKG2x/CD94 receptors recognize different HLA-E-restricted peptides, but binding studies have shown that the two most critical peptide contact points for huNKG2x/CD94 are positions P5, an invariant Arg, and P8, a variable hydrophobic residue in class I leaders (12, 15, 16). Based on the structure of MICA bound to NKG2D, Li and coworkers (17) proposed that NKG2A/CD94 would bind HLA-E with CD94 oriented over the α1 helix of HLA-E and C-terminal part of the peptide, and NKG2A over the α2 helix. Subsequent binding and mutagenesis studies of HLA-E helices (4, 12, 18) provided further support for this orientation, indicating CD94 is likely responsible for reading out the C terminus of the peptide. The structural basis for affinity differences between NKG2x/CD94 receptors has also not been conclusively determined, partly because of the high sequence similarity between these receptors. Here, we present the crystal structure of a complex between NKG2A/CD94 and HLA-E that directly answers these questions and suggests an alternate role for the activating NKG2C/CD94 receptor.

Results

Soluble forms of the ectodomains of NKG2A/CD94 and HLA-E were refolded *in vitro* from bacterial inclusion bodies (4). For crystallization, HLA-E was bound with the nonamer peptide derived from HLA-G (VMAPRTLFL), which binds NKG2x/CD94 with the highest affinity of any HLA-E/peptide combination so far tested (4). Initial phases were determined by molecular replacement using previously determined structures of CD94 (19) and HLA-E (10) as search models [supporting information (SI) Table S1]. The asymmetric unit (AU) contained two complete complexes of NKG2A/CD94–HLA-E. Despite the low resolution (d_{min} = 4.4 Å), electron density was continuous and interpretable throughout one of the two NKG2A

Author contributions: B.K.K., J.C.P., J.K., and R.K.S. designed research; B.K.K., J.C.P., and J.K. performed research; B.K.K., J.C.P., J.K., and R.K.S. analyzed data; and B.K.K., J.C.P., J.K., and R.K.S. wrote the paper.

The authors declare no conflict of interest.

*Present address: Structural Genomic Consortium (SGC), University of Toronto, Toronto, ON, Canada M5G 1L5.

†To whom correspondence should be addressed. E-mail: rstrong@fhcrc.org.

Data deposition: The atomic coordinates and structure factors have been deposited in the Protein Data Bank, www.pdb.org (PDB ID code 3CII).

This article contains supporting information online at www.pnas.org/cgi/content/full/0802736105/DCSupplemental.

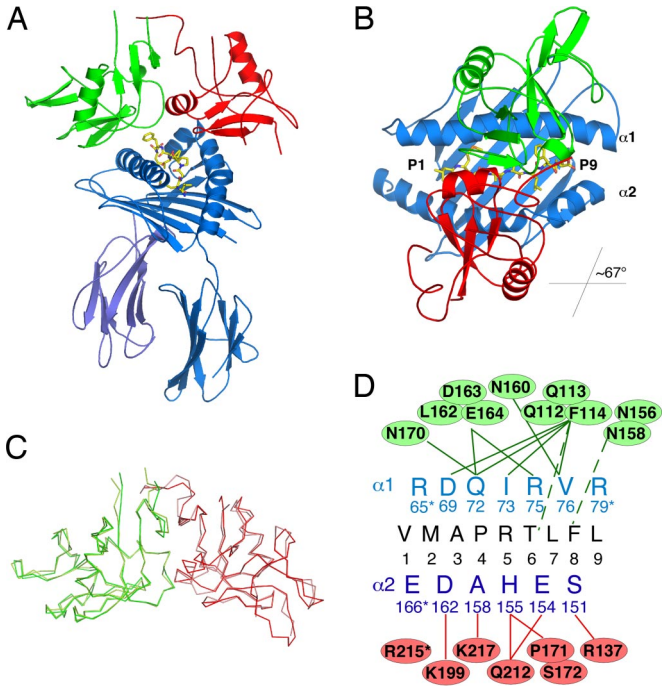

Fig. 1. The NKG2A/CD94/HLA-E complex structure. (*A* and *B*) Ribbon representations of the complex viewed from the side (*A*) or from above (*B*), colored by chain [NKG2A: red; CD94: green; HLA-E heavy chain: blue; β_2m: purple; peptide (showing all atoms): yellow]. (*C*) Superpositions of α-carbon backbone traces of NKG2A/CD94 crystallized in complex with HLA-E (showing the *de novo*-built NKG2A model; NKG2A: dark green; CD94: dark red) and alone (NKG2A: pale green; CD94: pale red; ref. 12). The superpositions were aligned on CD94. Note that the structure of the receptor in the complex includes residues 200–203 that are absent from the free structure. (*D*) A schematic representation of the contacts between NKG2A (red spheres)/CD94 (green spheres) and HLA-E α1 (light blue) and α2 (dark blue) domains. An asterisk indicates residues (HLA-E^{R65}, HLA-E^{R79}, HLA-E^{E166}, NKG2A^{R215}) that are predicted to be involved in binding by mutagenesis (12) but are not contacts in the structure.

molecules (Fig. S1), allowing a *de novo* chain trace (Fig. 1 *A–C*); the maps were of sufficient quality to unambiguously assemble complexes and assign approximate contacts (Fig. S1, Fig. 1*D*). The validity of our modeling, beyond reasonable refinement statistics (Table S1), is demonstrated by consistency with previous binding and modeling studies (4, 12, 17, 18) and good agreement between NKG2A/CD94 from our structure and its recently determined crystal structure (PDB ID code 3BDW) (12). The *de novo*-built NKG2A molecules from our structure superimpose with an rmsd of 0.59–0.60 Å with the NKG2A molecules from 3BDW. In addition, the NKG2A/CD94 receptor structure and our complex structure superimpose with rmsds of 0.76 to 0.86 Å (Fig. 1*C*), resulting in essentially identical pseudodyad axes relating NKG2A to CD94 (≈175°) free or bound to HLA-E. For our final structure, we replaced the *de novo*-built NKG2A moiety with its actual crystal structure primarily to improve the stereochemistry, because the difference in refinement statistics using the *de novo* model or 3BDW was modest. Despite application of noncrystallographic symmetry (NCS) restraints throughout refinement, the orientation of the two NKG2A/CD94 receptors on their respective HLA-E ligands differs significantly (by ≈5°), indicating some flexibility in binding. We also note that the overall orientation of receptor on ligand, ≈67° (Fig. 1*B*), is more orthogonal than predicted by previous modeling attempts, at ≈40° (12).

In the receptor, two elements are primarily responsible for the formation of the interface between NKG2A and CD94 (Fig. 2). One is formed on the membrane-proximal (N-terminal) face of the heterodimer where β-strand 1 (β1) from both NKG2A and CD94 bridges the dimer interface and joins β-sheet 1 (β1, β2, and β7) of each monomer into an extended β-sheet containing a total of six β-strands. The second region of the heterodimer interface is formed by CD94 residues 107–111 (sequence: MFSSS) and NKG2A residues 168–171 (sequence: IISP), which are just C-terminal to the second α-helix of NKG2A.

In the complex, CD94 binds over the α1 helix of HLA-E and unambiguously contributes all contacts to the C-terminal portion of the peptide, whereas NKG2A sits over the over the α2 helix (Fig. 3*A*). The interface between NKG2A/CD94 and HLA-E/peptide buries ≈2,600 Å^2, with CD94 accounting for ≈1,400 Å^2 and NKG2A ≈1,200Å^2. Two stretches of CD94 residues make significant contacts with the HLA-E platform: CD94^{Q112}, CD94^{Q113}, and CD94^{F114}, which are directly adjacent to the interface with NKG2A; and CD94^{N160}, CD94^{L162}, CD94^{D163}, and CD94^{E164}. CD94^{F114} and CD94^{L162} bind to a hydrophobic patch that includes HLA-E^{V76}, HLA-E^{I73}, and P8^{Phe} of the peptide

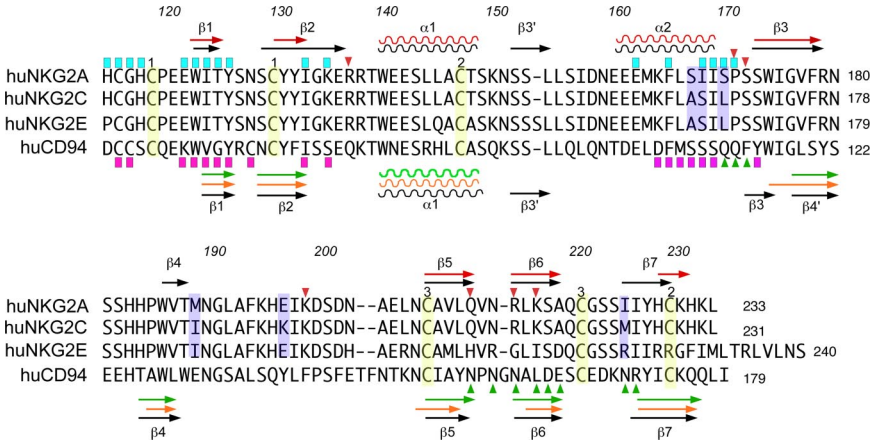

Fig. 2. Sequence alignment of human NKG2x receptors. NKG2A secondary structural elements from the complex (red) and free (black) structures are shown above the sequences (β-sheets: arrows; α-helices as wavy lines); CD94 secondary structure elements from the complex (green), NKG2A/CD94 free (3BDW, black), and CD94 alone structures (1BSE, orange) are shown below. In addition, CD94 residues that bind HLA-E/peptide are indicated by green triangles; NKG2A residues that bind HLA-E/peptide by red triangles; CD94 residues contacting NKG2A by magenta rectangles; and NKG2A residues contacting CD94 by cyan rectangles. Residues in the alignments shaded blue highlight sequence differences between NKG2A and NKG2C. Paired cysteine residues in NKG2A that form intrachain disulfide bonds are numbered above the alignments from 1 to 3.

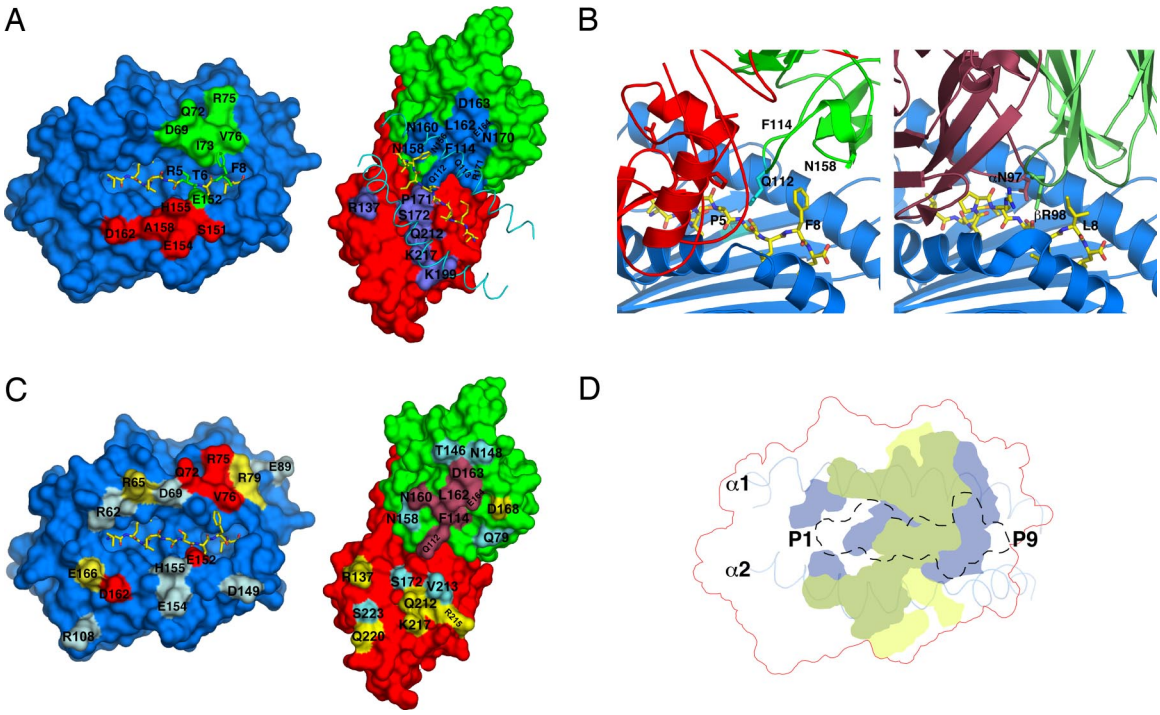

Fig. 3. Contacts between NKG2A/CD94 and HLA-E/peptide. (*A*) Molecular surface representations are shown of NKG2A (red), CD94 (green), and HLA-E (blue), with the peptide shown in an all-atom representation (N terminus on the left). The complex has been splayed open to reveal the interface, with regions on each half of the complex colored by the molecule making reciprocal contacts. Coils have been included on the right to indicate the position of the HLA-E α-helices from the complex relative to NKG2A/CD94. (*B*) Contacts between NKG2A/CD94 (*Left*) or TCR KK50.4 (*Right*) and HLA-E are shown, with the molecules shown as ribbons, colored as in *A*. The TCR α chain is purple, and the TCR β chain is green. (*C*) The complex is shown as in *A*, but with interface residues colored by a heat map (mutations with >10-fold effect on affinity: red for HLA-E or salmon for CD94; 3- to 5-fold effect: yellow; 2-fold or less: blue) based on the previous alanine mutagenesis analysis (12). (*D*) Schematic representation of the binding footprints of NKG2A/CD94 (yellow) and TCR KK50.4 (blue) on HLA-E.

(Fig. 3*B*). Other CD94 residues that contribute contacts include $CD94^{N156}$, $CD94^{D158}$, and $CD94^{N170}$. Considering the modest resolution of our structure, with appropriately conservative modeling of NKG2A side-chains, it is still clear that $NKG2A^{R137}$, $NKG2A^{P171}$, $NKG2A^{K199}$, $NKG2A^{Q212}$, and $NKG2A^{K217}$ contact HLA-E residues $HLA\text{-}E^{S151}$, $HLA\text{-}E^{E154}$, $HLA\text{-}E^{H155}$, $HLA\text{-}E^{A158}$, and $HLA\text{-}E^{D162}$. $CD94^{Q112}$ makes the most extensive peptide contacts of any CD94 residue by intercalating into the peptide between $P5^{Arg}$ and $P8^{Phe}$, although clear density for the side-chain of $P5^{Arg}$ is absent, making confident assignment of contacts to this residue difficult. $CD94^{Q112}$ is in closest proximity to peptide position $P6^{Thr}$, interacting with the peptide backbone as this side-chain is buried in HLA-E. $CD94^{N156}$ and $CD94^{N158}$ are part of a loop that abuts $P8^{Phe}$. Sullivan and coworkers (12) reported that a $CD94^{N158A}$ mutation actually increased binding to HLA-E ≈3-fold, supporting a direct, main-chain interaction between $CD94^{N158}$ and $P8^{Phe}$.

Mapping receptor/ligand interface contacts in our structure is largely consistent with previous mutagenesis studies (12, 18), predicting that all residues that, when mutated, decrease affinity by 10-fold or more are also direct contacts ($HLA\text{-}E^{Q72}$, $HLA\text{-}E^{R75}$, $HLA\text{-}E^{V76}$, $HLA\text{-}E^{E152}$, $HLA\text{-}E^{D162}$, $CD94^{Q112}$, $CD94^{Q114}$, $CD94^{N160}$, $CD94^{162}$, $CD94^{D163}$, $CD94^{E164}$; Fig. 3*C*). Residues that show more modest 3- to 4-fold affinity decreases when mutated ($NKG2A^{Q220}$, $NKG2A^{R215}$, $HLA\text{-}E^{R65}$, $HLA\text{-}E^{R75}$, $HLA\text{-}E^{E166}$; $CD94^{D168}$) do not appear to be direct contacts in our analysis. Several contacts in the complex structure ($HLA\text{-}E^{H155}$, $HLA\text{-}E^{D69}$, $NKG2A^{S172}$) only demonstrated a modest (≈2-fold) decrease in affinity when mutated, suggesting that these residues do not contribute significantly to the ΔG of binding.

Individuals with the correct HLA haplotype can generate T cell receptors (TCRs) that specifically recognize HLA-E complexes presenting hCMV UL40-derived peptides (VMAPRTLIL) (20). Comparison of our structure with the complex crystal structure of one such TCR, KK50.4, bound to HLA-E demonstrates that the KK50.4 and NKG2A/CD94 footprints on HLA-E are essentially overlapping surfaces (Fig. 3*D*) (21). $CD94^{Q112}$ and KK50.4 residues βR98 and αN97 contact the peptide in comparable ways, intercalating between the side-chains of $P5^{Arg}$ and $P8^{Phe}$ and contacting the main-chain of $P6^{Thr}$ (Fig. 3*B*). NKG2A/CD94 buries more surface area than KK50.4 (≈2,600 Å^2 versus ≈2,150 Å^2), and consistent with this, the affinity of NKG2A/CD94 for HLA-E is considerably higher (≈1 μM vs. 30 μM).

Why does NKG2A/CD94 bind any given HLA-E/peptide complex with a ≈6-fold higher affinity than NKG2C/CD94, given their high sequence identity (95%), different at only six positions (Fig. 2)? Three of these differences are in a loop (NKG2A residues 167–170) that forms a significant part of the interface with CD94 (Fig. 2). Residues of both NKG2A and CD94 adjacent to this interface make significant contacts with HLA-E/peptide: CD94 residues 112–114 interact with both the peptide and α1 helix of HLA-E, and NKG2A residues P171 and S172 likely contact $HLA\text{-}E^{H155}$ and the peptide at $P5^{Arg}$. To test whether residues 167–170 account for the difference in affinity between NKG2A/CD94 and NKG2C/CD94, we swapped these residues between NKG2A and NKG2C (generating "$NKG2C^{triple}$" and "$NKG2A^{triple}$" variants) and tested the effect on affinity for two different HLA-E complexes by surface plasmon resonance (Table 1). The $NKG2C^{triple}$/CD94 mutant bound HLA-E with affinities nearly identical to those of wtNKG2A/CD94, whereas the $NKG2A^{triple}$/CD94 mutant bound with affinities much more similar to those of wtNKG2C/CD94. These results establish that NKG2x interface residues 167–170 indeed account for the difference in affinity between NKG2A/

Table 1. K_Ds in μM of NKG2A/C mutants

Mutant	HLA-E^{G*}	HLA-E^{b27†}	HLA-E^{Kpeptide‡}
wtNKG2A	0.8 ± 0.055	5.7 ± 0.4	12.4 ± 1.5
wtNKG2C	5.2 ± 0.2	18.2 ± 0.5	10.6 ± 1.2
NKG2C(165–168 SIIS)	0.9 ± 0.1	3.8 ± 0.1	
NKG2A(167–170 ASIL)	3.8 ± 0.3	12.9 ± 2.8	

*Peptide sequence is VMAPRTLFL.
†Peptide sequence is VTAPRTL*LL*.
‡Peptide sequence is VMAP*K*TLFL.

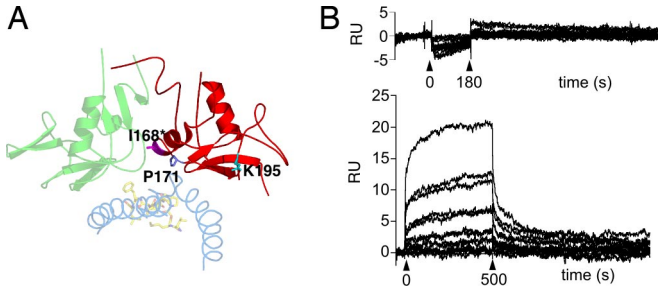

Fig. 4. NKG2C/CD94 binds to hCMV gpUL18. (*A*) Residues in NKG2A (Pro-171), NKG2C (Lys-195), or both (NKG2A^{I168}/NKG2C^{S166}, positions that are equivalent in the alignment, indicated by an asterisk) evolving under positive selection (i.e., with PAML scores of >0.95) are mapped onto the structure of NKG2A (red), shown in a ribbon representation. (*B*) SPR sensorgrams of the response of NKG2A/CD94 (*Upper*) and NKG2C/CD94 (*Lower*) analytes to chip-coupled gpUL18. Concentrations of NKG2A/CD94 are 1.6, 3.1, 6.3, 12.5, and 25.0 μM; concentrations of NKG2C/CD94 are 1.25, 2.5, 5, 10, 20, and 40 μM. Injection start and stop points are marked by arrows.

CD94 and NKG2C/CD94. Comparable results have also been reported by a recent study (12).

Because the NKG2x residues that account for the affinity difference form the interface with CD94 and do not appear to directly contact HLA-E/peptide, the affinity difference is likely due to adjustments in heterodimer orientation that indirectly alter interactions with HLA-E. Residues adjacent to the NKG2A–CD94 interface include NKG2A^{P171} and CD94^{Q112}, both of which potentially contact peptide P5^{Arg}. This raised the possibility that the P5^{Arg} also contributes to the affinity difference between NKG2A and NKG2C. To test this, we generated HLA-E, presenting the HLA-G nonamer with P5 mutated to Lys (VMAP*K*TLFL), and measured the binding affinity to NKG2A/CD94 and NKG2C/CD94. The affinities for both receptors were very similar (10 μM for NKG2A/CD94 and 12 μM for NKG2C/CD94; Table 1), confirming the importance of P5^{Arg} in contributing to both the overall affinity and the affinity differential between NK2A/CD94 and NKG2C/CD94.

Many immune receptors are targeted for immune evasion by viral and bacterial decoy ligands or mimetics and may be adaptively evolving to avoid such interactions. In this scenario, the immune receptors would be evolving under positive selection, meaning that nonsynonymous, or sequence-altering, changes would be favored. To look for signatures of positive selection in the *NKG2A* and *NKG2C* genes, we analyzed gene sequences from primate species spanning >35 million years of evolution and found that the sequence data for both genes fit a codon model that permits positive selection (Nsites model M7; $P = 0.002$ for NKG2A, $P = 0.006$ for NKG2C). This indicates that both *NKG2A* and *NKG2C* have evolved under positive selection, suggesting that both genes have been actively engaged in a host-pathogen conflict throughout primate evolution. In contrast, a similar evolutionary analysis of CD94 in primates did not reveal any evidence of positive selection. The identification of specific amino acid residues in NKG2A and NKG2C that are evolving under recurrent positive selection can implicate the amino acid residues or domains that directly interact with the pathogen-derived protein. Using two different methods (the NSsites models and REL analysis), we identified two NKG2A and two NKG2C ectodomain codons as having repeatedly evolved under positive selection (Fig. 4*A*): NKG2A^{I168} (0.9998, 283); NKG2A^{P171} (0.99, not identified); NKG2C^{S166} (0.95, 446); and NKG2C^{K195} (0.95, 329); where the numbers in parentheses correspond to the individual probabilities (BEB posterior probability, from NSsites; ref. 22) and Bayes factor (from REL; ref. 23), respectively. All codons listed had a posterior probability >95% in NSsites. These results are particularly intriguing because NKG2A^{I168}, NKG2A^{P171}, and NKG2C^{S166} lie at the interface with CD94 and are critical to determining the overall affinity of the interaction with HLA-E. NKG2C codon 195, on the other hand, is distant from the HLA-E interacting surface.

Because of the strong signals of positive selection in HLA-E interacting residues, we hypothesized that NKG2x/CD94 receptors may also interact with a pathogen-derived ligand. Potential candidates included two MHC-related CMV proteins, gpUL142 and gpUL18. gpUL18, which like class I MHC associates with β_2-microglobulin (β_2m) and peptide, binds with very high affinity (K_D in the low nM range) to the inhibitory NK receptor LIR1/ILT2/CD85j (24, 25). Several recent studies, although circumstantial, have suggested the possibility of direct interactions between NKG2C/CD94 and CMV-encoded proteins, including gpUL18 (26, 27). In our assessment of this possibility, surface plasmon resonance binding studies, in which glycosylated gpUL18 was chip-coupled, clearly demonstrate an interaction between NKG2C/CD94 and gpUL18, but not between NKG2A/CD94 and gpUL18 (Fig. 4*B*). Although we cannot satisfactorily fit these data with appropriate binding models (possibly because of heterogeneity in this preparation of the heavily glycosylated gpUL18 protein), precluding quantitation, the interaction is likely to be weak, with a K_D in the 10- to 100-μM range The use of the same gpUL18-coupled surface for both receptors provided an internal binding control. This result confirms the possibility that NKG2x/CD94 receptors are under positive selection because of genetic conflict with pathogen-associated proteins.

Discussion

Low resolution structures can be a rich source of information, providing valuable insight into biological questions (28). Despite the low resolution of this analysis, the NKG2A/CD94–HLA-E complex structure reveals important details about the recognition mechanism of this important family of immunoreceptors, accounting for affinity differences between NKG2A and NKG2C for HLA-E and between different peptides for NKG2x receptors. Sequence differences in NKG2x residues 167–170, which form part of the heterodimer interface, account for the affinity difference between NKG2A/CD94 and NKG2C/CD94 for given HLA-E/peptide complexes. Although a crystal structure of NKG2C/CD94 is not yet available for comparison, we hypothesize that these interface residues indirectly affect ligand affinity through changes in the overall arrangement of domains in NKG2x/CD94 receptors. In order for this mechanism to explain observed affinity differences, NKG2x/CD94 receptors should be relatively rigid, unlike NKG2D homodimers, which show significant interface flexibility (29, 30). The near-perfect superimposability of the ligand-bound and free states of NKG2A/CD94 supports such a conclusion. Studies of the murine C-type lectin-like Ly49 family of receptors, which function as homodimers in binding to MHC ligands, have also demonstrated that residues at the homodimer interface critically affect ligand binding (31–33).

Our comparative analysis across primate species revealed that both NKG2A and NKG2C are evolving under strong positive selection, consistent with involvement in a host–pathogen conflict. We note that this is not the only possible explanation of the data. However, residues encoded by codons with the highest signal for positive selection lie either in (or near) the HLA-E binding surface or in the NKG2x/CD94 interface (with the exception of NKG2C^{K195}), positions that may affect ligand interactions directly or indirectly. In support of the host–pathogen conflict hypothesis, direct binding studies do show a specific, although weak, interaction between a likely extant candidate, hCMV gpUL18 and NKG2C/CD94, although not between NKG2A/CD94 and gpUL18. The nature of this interaction suggests that NKG2x/CD94 receptors may directly interact with virally encoded proteins, possibly hCMV gpUL18 or related proteins, either as part of a viral immunoevasion strategy, usurping the inhibitory receptor NKG2A/CD94 as gpUL18 appears to subvert LIR1, or as an immune system response to such an evasion strategy, by directly engaging the activating receptor NKG2C/CD94.

Materials and Methods

Protein Expression and Purification. Human NKG2A (residues 99–233 plus an N-terminal 6× His tag) and CD94 (residues 31–179) were both expressed and purified as described (4). Mutations in NKG2A and NKG2C were introduced by using the QuikChange procedure (Stratagene). For crystallography, NKG2A/CD94 was additionally digested overnight at room temperature with bromelain (Calbiochem) at a ratio of 30:1. The HLA-E complex, containing a nonamer peptide derived from the leader sequence of HLA-G (VMAPRTLFL), was refolded by dilution as described (10) and purified by size exclusion and ion exchange chromatography to separate complexes from free heavy chains. For the final step of purification, NKG2A/CD94 and HLA-E were copurified by size exclusion chromatography.

Crystallography. NKG2A/CD94–HLA-E complex was concentrated to 4.0 mg/ml and crystallized by hanging drop vapor diffusion at 18°C by mixing equivalent volumes of protein solution and reservoir buffer [1.8 M $(NH_4)_2SO_4$, 0.3–0.7% sucrose, 100 mM Tris (pH 8.0)], with crystals typically forming after 2–4 weeks. Crystals were dehydrated by transferring the coverslip to a well containing 3.0 M $(NH_4)_2SO_4$ and 100 mM Tris (pH 8.0) overnight and were cryopreserved in well solution plus 25% sucrose wt/wt in liquid nitrogen.

X-ray data were collected at the Advanced Light Source (Berkeley, CA), beamline 8.2.2, and were processed with DENZO/Scalepack; phases were determined by molecular replacement using AMoRe, as implemented in the CCP4 suite of programs (34), with HLA-E (1KPR.pdb) and a CD94 monomer (1B6E.pdb) as independent search models. Initial phases were improved by using the density modification program DM (CCP4 suite). A homology model of NKG2A based on the structure of CD94 was placed into the electron density manually by using COOT (35) and rebuilt according to the electron density. When submitted to the DALI server (36), this partially built NKG2A identified DC-SIGN (1SL6.pdb) as the closest structural homolog of NKG2A. DC-SIGN was then used as a reference molecule to complete the first NKG2A molecule. This first NKG2A/CD94 complex was docked onto the second HLA-E molecule, creating our first model for the entire AU, encompassing two complete complexes. A TLS restrained refinement was performed, which improved R_{work} to 0.34 and R_{free} to 0.38. We completed our model with minimal manual building into regions where density was unequivocal. Our completed refined structure showed an overall R value of 0.33 and R_{free} of 0.37. Recently the structure of NKG2A/CD94 by itself was published (3BDW.pdb). We carried out a further round of rigid body refinement using the NKG2A coordinates from this structure, with a final R value of 32.2 and R_{free} of 35.5. NCS restraints were imposed throughout refinement.

Our initial solvent-flattened map, which was unbiased with respect to NKG2A, showed structural features not easily predicted from sequence analysis alone. We attempted to use CD94 and NKG2D, the two closest matches in terms of sequence identity, to generate our initial NKG2A model. However, based on a DALI search the electron density of NKG2A more closely resembled DC-SIGN, CD69 and tetranectin, all lectin or lectin-like proteins with lower sequence identity to NKG2A, most likely because of the second α-helix present in these molecules but not in CD94. The moderately high crystallographic R factors of our final model are likely due to a combined effect of the low resolution of the crystal and its high intrinsic disorder. We have tabulated statistics for the 32 structures deposited in the PDB within the last 5 years that have resolution in the range of 3.9–4.1 Å. The average R_{free} for these structures is 0.35, and average R_{work} is 0.32 (medians are 0.35/0.31). The R_{free} ranges from 0.25 to 0.50, and the R_{work} ranges from 0.20 to 0.49, showing that our model is comparable in quality to the standard in this resolution range.

Interaction Analysis. Surface plasmon resonance (SPR) measurements were carried out on Biacore3000 instrumentation. All proteins used for SPR were repurified by SEC in HBS-EA buffer (Biacore) within 48 h of use. Protein concentrations were determined by bicinchoninic acid protein assay (Pierce), with associated errors $\leq$2%. Affinity interactions between NKG2x/CD94 and HLA-E were carried out as described (4). To assess the gpUL18-NKG2x/CD94 interaction, $\approx$1,000 response units gpUL18 was amine coupled to a CM sensor chip as described (24); NKG2A/CD94 and NKG2C/CD94 were used as analytes.

Evolutionary Analysis. Multiple sequence alignments for NKG2A and NKG2C for available primate sequences were generated with Clustal_X (37). Accession numbers for primate *NKG2A* genes include AF461812 (*Homo sapiens*), AF350005 (*Pan troglodytes*), AF190979 (*Macaca mulatta*), AJ585528 (*Macaca fasicularis*), EF426674 (*Papio anubis*), AF470391 (*Pongo pygmaeus*), EF050432 (*Callithrix jacchus*), and EU024495 (*Saimiri sciureus*). Accession numbers for primate *NKG2C* genes include AJ001684 (*H. sapiens*), AF259057 (*P. troglodytes*), AJ585531 (*M. mulatta*), AJ585530 (*M. fasicularis*), EF050434 (*C. jacchus*), and EU024496 (*S. sciureus*). Additional primate sequences for the *NKG2C* gene were obtained by performing BLAST inquiries of the Trace Archives for *Gorilla gorilla*, *Papio hamadryas*, and *Pongo pygmaeus abelii*. A maximum likelihood analysis was performed with codeml from the PAML 3.14 software package (22). To detect the selective pressures shaping the evolution of each gene, we fit the multiple alignments to an NSsites model that allowed positive selection (M8) or disallowed positive selection (M7), assuming the F3 × 4 model of codon frequencies. Likelihood ratio tests were performed to determine whether allowing the codons to evolve under positive selection would give a significantly better fit for the data. To identify specific codons that have undergone recurrent positive selection, we used the NSsites model in codeml from PAML 3.14 (22). To confirm the sites identified by the NSsites approach, we also used the random effects method (REL) from the web-based DataMonkey package, with the Bayes significance factor cutoff set at 50 (23).

ACKNOWLEDGMENTS. We thank Pamela J. Bjorkman (California Institute of Technology) for the kind gift of UL18 protein and Stephen Maley for suggesting and assisting with the phylogenetic analyses. B.K.K. was the recipient of a postdoctoral fellowship from the Cancer Research Institute, New York. J.K. was funded by a grant from Puget Sound Partners for Global Health. This work was supported by National Institutes of Health Grant AI48675.

1. Natarajan K, Dimasi N, Wang J, Mariuzza RA, Margulies DH (2002) Structure and function of natural killer cell receptors: Multiple molecular solutions to self, nonself discrimination. *Annu Rev Immunol* 20:853–885.
2. Braud VM, *et al.* (1998) HLA-E binds to natural killer cell receptors CD94/NKG2A, B and C. *Nature* 391:795–799.
3. Lee N, *et al.* (1998) HLA-E is a major ligand for the natural killer inhibitory receptor CD94/NKG2A. *Proc Natl Acad Sci USA* 95:5199–5204.
4. Kaiser BK, *et al.* (2005) Interactions between NKG2x immunoreceptors and HLA-E ligands display overlapping affinities and thermodynamics. *J Immunol* 174:2878–2884.
5. Arase H, Mocarski ES, Campbell AE, Hill AB, Lanier LL (2002) Direct recognition of cytomegalovirus by activating and inhibitory NK cell receptors. *Science* 296:1323–1326.
6. Smith HR, *et al.* (2002) Recognition of a virus-encoded ligand by a natural killer cell activation receptor. *Proc Natl Acad Sci USA* 99:8826–8831.
7. Borrego F, Ulbrecht M, Weiss EH, Coligan JE, Brooks AG (1998) Recognition of human histocompatibility leukocyte antigen (HLA)-E complexed with HLA class I signal sequence-derived peptides by CD94/NKG2 confers protection from natural killer cell-mediated lysis. *J Exp Med* 187:813–818.
8. Llano M, *et al.* (1998) HLA-E-bound peptides influence recognition by inhibitory and triggering CD94/NKG2 receptors: Preferential response to an HLA-G-derived nonamer. *Eur J Immunol* 28:2854–2863.
9. O'Callaghan CA, *et al.* (1998) Structural features impose tight peptide binding specificity in the nonclassical MHC molecule HLA-E. *Mol Cell* 1:531–541.
10. Strong RK, *et al.* (2003) HLA-E allelic variants. Correlating differential expression, peptide affinities, crystal structures, and thermal stabilities. *J Biol Chem* 278:5082–5090.
11. Vales-Gomez M, Reyburn HT, Erskine RA, Lopez-Botet M, Strominger JL (1999) Kinetics and peptide dependency of the binding of the inhibitory NK receptor CD94/NKG2-A and the activating receptor CD94/NKG2-C to HLA-E. *EMBO J* 18:4250–4260.

12. Sullivan LC, *et al.* (2007) The heterodimeric assembly of the CD94-NKG2 receptor family and implications for human leukocyte antigen-E recognition. *Immunity* 27:900–911.
13. Tomasec P, *et al.* (2000) Surface expression of HLA-E, an inhibitor of natural killer cells, enhanced by human cytomegalovirus gpUL40. *Science* 287:1031.
14. Ulbrecht M, *et al.* (2000) Cutting edge: The human cytomegalovirus UL40 gene product contains a ligand for HLA-E and prevents NK cell-mediated lysis. *J Immunol* 164:5019–5022.
15. Kraft JR, *et al.* (2000) Analysis of Qa-1. (b) peptide binding specificity and the capacity of CD94/NKG2A to discriminate between Qa-1-peptide complexes. *J Exp Med* 192:613–624.
16. Miller JD, *et al.* (2003) Analysis of HLA-E peptide-binding specificity and contact residues in bound peptide required for recognition by CD94/NKG2. *J Immunol* 171:1369–1375.
17. Li P, *et al.* (2001) Complex structure of the activating immunoreceptor NKG2D and its MHC class I-like ligand MICA. *Nat Immunol* 2:443–451.
18. Wada H, Matsumoto N, Maenaka K, Suzuki K, Yamamoto K (2004) The inhibitory NK cell receptor CD94/NKG2A and the activating receptor CD94/NKG2C bind the top of HLA-E through mostly shared but partly distinct sets of HLA-E residues. *Eur J Immunol* 34:81–90.
19. Boyington JC, *et al.* (1999) Structure of CD94 reveals a novel C-type lectin fold: Implications for the NK cell-associated CD94/NKG2 receptors. *Immunity* 10:75–82.
20. Pietra G, *et al.* (2003) HLA-E-restricted recognition of cytomegalovirus-derived peptides by human $CD8^+$ cytolytic T lymphocytes. *Proc Natl Acad Sci USA* 100:10896–10901.
21. Hoare HL, *et al.* (2006) Structural basis for a major histocompatibility complex class Ib-restricted T cell response. *Nat Immunol* 7:256–264.
22. Yang Z (1997) PAML: A program package for phylogenetic analysis by maximum likelihood. *Comput Appl Biosci* 13:555–556.
23. Pond SL, Frost SD (2005) DataMonkey: Rapid detection of selective pressure on individual sites of codon alignments. *Bioinformatics* 21:2531–2533.
24. Chapman TL, Heikeman AP, Bjorkman PJ (1999) The inhibitory receptor LIR-1 uses a common binding interaction to recognize class I MHC molecules and the viral homolog UL18. *Immunity* 11:603–613.
25. Cosman D, *et al.* (1997) A novel immunoglobulin superfamily receptor for cellular and viral MHC class I molecules. *Immunity* 7:273–282.
26. Guma M, *et al.* (2006) Expansion of CD94/NKG2C+ NK cells in response to human cytomegalovirus-infected fibroblasts. *Blood* 107:3624–3631.
27. Prod'homme V, *et al.* (2007) The human cytomegalovirus MHC class I homolog UL18 inhibits LIR-1^+ but activates LIR-1^- NK cells. *J Immunol* 178:4473–4481.
28. DeLaBarre B, Brunger AT (2006) Considerations for the refinement of low-resolution crystal structures. *Acta Crystallogr D* 62:923–932.
29. McFarland BJ, Kortemme T, Yu SF, Baker D, Strong RK (2003) Symmetry recognizing asymmetry: Analysis of the interactions between the C-type lectin-like immunoreceptor NKG2D and MHC class I-like ligands. *Structure (London)* 11:411–422.
30. McFarland BJ, Strong RK (2003) Thermodynamic analysis of degenerate recognition by the NKG2D immunoreceptor: Not induced fit but rigid adaptation. *Immunity* 19:803–812.
31. Kielczewska A, Kim HS, Lanier LL, Dimasi N, Vidal SM (2007) Critical residues at the Ly49 natural killer receptor's homodimer interface determine functional recognition of m157, a mouse cytomegalovirus MHC class I-like protein. *J Immunol* 178:369–377.
32. Lian RH, Li Y, Kubota S, Mager DL, Takei F (1999) Recognition of class I MHC by NK receptor Ly-49C: Identification of critical residues. *J Immunol* 162:7271–7276.
33. Wang J, *et al.* (2002) Binding of the natural killer cell inhibitory receptor Ly49A to its major histocompatibility complex class I ligand. Crucial contacts include both H-2Dd AND beta 2-microglobulin. *J Biol Chem* 277:1433–1442.
34. Collaborative Computational Project, Number 4 (1994) The CCP4 suite: Programs for protein crystallography. *Acta Crystallogr D* 50:760–763.
35. Emsley P, Cowtan K (2004) Coot: Model-building tools for molecular graphics. *Acta Crystallogr D* 60:2126–2132.
36. Holm L, Sander C (1994) The FSSP database of structurally aligned protein fold families. *Nucleic Acids Res* 22:3600–3609.
37. Thompson JD, Gibson TJ, Plewniak F, Jeanmougin F, Higgins DG (1997) The CLUSTAL_X windows interface: Flexible strategies for multiple sequence alignment aided by quality analysis tools. *Nucleic Acids Res* 25:4876–4882.